Optimal Signal Discrimination in a Low Signal-to-Noise Ratio Environment

Thiago Ciodaro, on behalf of the
ATLAS Tile Calorimeter Group.
Federal University of Rio de Janeiro
Rio de Janeiro, RJ, Brazil.
Email: ciodaro@cern.ch

***Abstract*— Energy measurements from calorimeter information are very important for particle detection in high-energy physics experiments. Calorimeters have a very good energy resolution, but some interesting particles produce a signal rather close to electronic noise values. This work presents the development of optimal signal discriminators to be implemented in a low signal-to-noise environment. They use signals from a highly segmented calorimeter (TileCal), which was built in the context of the ATLAS experiment for the Large Hadron Collider, operating at the European Organization for Nuclear Research (CERN).**

I. Introduction

Signal discrimination under low signal-to-noise ratio (SNR) conditions is required in many applications. In particular, in high-energy particle collider experiments, some subatomic particles produced in particle collisions interact with matter in the detectors such that the produced electrical signals are severely affected by noise. Robust detection strategies must be employed to correctly separate the interesting signal from the background noise [1].

ATLAS [2] is a particle detector operating at the Large Hadron Collider (LHC) at CERN. In order to extract interesting signatures characteristic of the particle collision products at LHC, ATLAS is divided into three subsystems: the inner detector, responsible for tracking particles, the calorimeters, responsible for the energy measurements [3] and the muon spectrometer, responsible for muon identification and tracking.

The readout of the ATLAS detector produces 1.5 MB of information per event. Considering the LHC's design collision rate (40 MHz), the total data rate is $\sim$ 60 TB/s [4]. The research focus being on well known physics signatures, an online filtering scheme was conceived, referred to as the trigger system. The ATLAS online trigger system is implemented in three cascaded levels, each possessing its own maximum event rate and latency time (time elapsed between the information arrival and the trigger decision). In particular, the first level (L1) is addressed in this work. The L1 trigger is based only on the compacted information from the calorimeter and the muon spectrometer [4]. It is fully implemented in hardware and it must reduce the event rate from 40 MHz to $\sim$ 100 kHz, taking no more than 2.5 μs per event.

Despite the fact that ATLAS has powerful muon detectors, muon identification from calorimeters can be used to reduce background fake triggers at L1 [5]. When muons interact with matter, the calorimeter signals produced have an intrinsic low SNR.

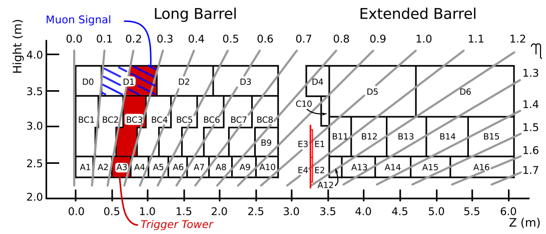

Fig. 1. The TileCal cell geometry.

This work presents the development of optimal signal discriminators for muon identification based on the information provided by the ATLAS barrel hadronic calorimeter (TileCal). Signals from TileCal are transmitted to a muon receiver, which interfaces with the ATLAS L1 muon trigger. The receiver sums topologically the received muon signals and performs optimal signal detection.

The paper is organized as follows. Section II briefly describes the TileCal, while Section III refers to the muon receiver design. Section IV discusses a matched filter based discriminator system and Section V presents simulation results for the discriminator performance. Finally, conclusions are summarized in Section VI.

II. The Tile Calorimeter

The TileCal consists of steel plates as absorber and plastic scintillating tiles as active sampling material, split into 64 modules in ϕ[1]. The tiles in each module are grouped together into readout cells (see Figure 1). Charged particles make the plastic tiles scintillate [6], while wave-length shifting fibers collect the scintillation light and transport it to a photomultiplier tube (PMT). The PMT converts the light into an electrical signal, whose amplitude is proportional to the deposited energy. After pulse shaping, the electrical signal is readout by the front-end electronics [7]. Each tile/cell is connected to two different PMTs and readout channels, which provides redundancy to the data acquisition.

The TileCal L1 interface card processes two readout signals [8]: a trigger tower signal (shaded region on Figure 1,

[1] ϕ is the azimuthal angle on the plane perpendicular to the beam axis (z)

spanning 0.1x0.1 on the $\eta \times \phi$ plane[2], which is used by the calorimeter trigger, and the muon signal, which is formed by the amplification of the last calorimeter layer (D cells) readout.

Currently, the TileCal muon signals are not being used by L1, but they are available at the trigger patch-panel and are being considered for a L1 upgrade.

III. Muon Receiver

Envisaging L1 muon performance improvement, a receiver system for the TileCal muon signals is being designed [9]. The main goal is to make a coincidence with the L1 muon trigger in order to reduce an unforeseen high fake trigger rate due to radiation background [10].

In order to increase the SNR, a sum of analog muon signals from the same D cell is evaluated before signal digitization. Nevertheless, while the tower signal provided by the TileCal has a SNR of $\sim$ 44 (which translates into $\sim$ 100 % efficiency against noise), the summed muon signal has a SNR of $\sim$ 3.1 [11].

The muon receiver digitizes the summed muon signal at 40 MHz, with an 8-bit ADC. The final digital word is read by a FPGA, where the signal discriminators must be implemented.

IV. Signal Discriminators

It is well-known in signal theory that a matched filter [12] is the optimal linear discriminator with respect to SNR. This discriminator bases its decision on two hypotheses for the received signal: H_0, there is no signal and only noise is received; H_1, the signal of interest is present, together with additive noise. The likelihood of the two hypotheses is defined as the ratio between the joint probability density function (*pdf*) of the received signal in both hypotheses, and it is the best measurement of how likely a received signal is from H_1 or H_0.

$$\Lambda(\mathbf{r}) \triangleq \frac{pdf_{\mathbf{r}|H_1}(\mathbf{r})}{pdf_{\mathbf{r}|H_0}(\mathbf{r})} \underset{H_0}{\overset{H_1}{\gtrless}} \gamma \tag{1}$$

where $pdf_{\mathbf{r}|H_n}(\mathbf{r})$ is the *pdf* of the received signal $\mathbf{r}$ under hypothesis n.

Two versions of the matched filter discriminators are discussed here. A simplified approach considers the muon signal well represented by the signal corresponding to the mean energy deposited by the muon. This simplification aims at reducing the discriminator complexity, which is quite attractive for online implementation. A full stochastic matched filter design considers, for simplicity, both muon and noise signals to be Gaussian processes.

A. Simplified Approach

Considering that the TileCal readout noise is a zero-mean Gaussian ($w(t)$), the received signal ($r(t)$) in both hypotheses is:

$$H_0 : r(t) = w(t), \qquad H_1 : r(t) = m(t) + w(t) \tag{2}$$

where $m(t)$ is the mean muon signal. Considering that the noise is white, the likelihood in Equation 1 can be simplified to:

$$\Lambda(r(t)) = \int r(t)m(t) \tag{3}$$

B. Stochastic Approach

The full stochastic design can be simplified if the signals of interest, besides the noise, are considered Gaussian [13]. Though this condition is not always true, it may be assumed for the sake of simplicity.

The Karhunen-Loève representation of a stochastic process is applied, resulting in a finite set of constants (λ_i) and orthonormal functions ($e_i(t)$), which are, respectively, the eigenvalues and eigenfunctions of the autocovariance function of the given stochastic process [14]. A signal from the stochastic process ($r(t)$) can be mapped onto this representation without loss of information:

$$\begin{aligned} r_i &= \int r(t)\phi_i(t)dt \\ r(t) &= \sum_{i=0}^{K} r_i \phi_i(t) \end{aligned} \tag{4}$$

the coefficients r_i are uncorrelated and, as they are Gaussian, independent. In this way, the received signals are mapped onto the eigenfunctions $e_i(t)$ and the likelihood in Equation 1, after some simplifications can be calculated as:

$$\begin{aligned} \Lambda(r(t)) &= \frac{1}{N_0} \iint r(t) \left[\sum_{i=0}^{K} \lambda_i d_i\right] r(u)\ du\ dt \\ &\quad + \iint m(t) \left[\sum_{i=0}^{K} d_i\right] r(u)\ du\ dt \end{aligned} \tag{5}$$

where $d_i = (\lambda_i + N_0/2)^{-1}\phi_i(t)\phi_i(u)$ and $N_0/2$ is the noise spectral density. Again, $m(t)$ is the average muon signal. Also, this approach requires the input noise to be white.

C. Implementations

During the detector commissioning phase, experimental tests with muon beams impinging on the calorimeter in fixed η positions were done to evaluate the detector's performance [11]. A special setup was implemented to digitize the TileCal muon signals. Further, these signals were used to simulate, in PSpice [15], the receiver's digitized signal.

The simulated digitized summed signals were used to develop the signal discriminators described above. Data were split into two sets: development and test. While the development set is used to design the discriminator, the test evaluates its performance and generalization capability. In total, almost 20,000 signals from muons were considered (at different η), and more than 20,000 noise signals for the respective cell

[2]The pseudorapidity η is defined as $\eta = -\ln\left(\tan\frac{\theta}{2}\right)$, where θ is the polar angle measured from the beam axis (z)

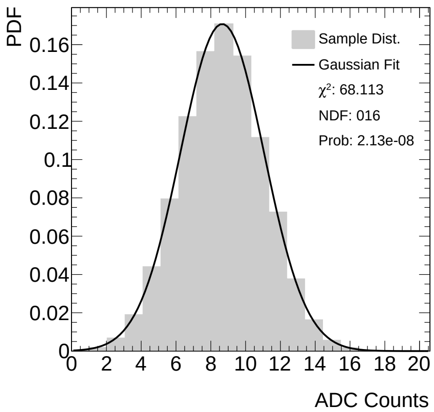

Fig. 2. Gaussian fit for digitized noise samples, for the D1-cell.

readouts. Each signal contains 11 digitized samples, in 8-bit resolution, as provided by the muon receiver.

Performance was evaluated by the maximum SP index[3]. This performance measure allows ballancing detection efficiency and false alarm rate, as it considers a geometrial mean of both detection probabilities (signal and noise) [16].

The TileCal readout noise is not fully white. This requires a whitening stage to be employed and applied to the received signals. Also, the Gaussian hypothesis for the TileCal readout noise was submitted to a χ^2 test. Figure 2 shows the noise samples distribution and the respective Gaussian fit. This result accumulates noise samples from the D cell at $\eta = 0.15$ and $\eta = 0.25$ (D1 cell in Figure 1).

Despite the reasonable Gaussian behavior, the χ^2 test rejected the Gaussian model. Thus, the Kullback-Leibler divergence [17], as a measurement of similarity between two distributions, was employed. The Jensen-Shannon test [17] goes between zero, for completely different distributions, and one, for similar distributions. In order to compare to the Gaussian model, a distribution with the same number of noise observations was obtained from a random Gaussian generator, keeping the same mean and variance as for the noise sample distribution. The test returned 0.997, for the D1 cell, and 0.999 for the D2 cell (η = 0.35 and 0.45), indicating that the noise samples distribution are not far from a Gaussian model.

For the muon signal, each sample was compared to the Gaussian model as above, by means of the Jensen-Shannon test (see Table I, for muons impinging on the calorimeter at η = 0.15). Values close to one indicate that the evaluated muon sample mainly consists of noise (as both distributions are similar), while values close to zero indicate that the effect of a muon crossing the calorimeter is more probable. The results indicate that samples in the middle of the pulse (s_5 to s_7) are less similar to noise, as expected from the normalized muon pulse shape [11] (see Figure 3). Samples near to the pulse baseline are more affected by noise than samples closer

[3]SP = $\sqrt{\sqrt{P_m P_n}\left(\frac{P_m+P_n}{2}\right)}$, where P_m stands for the probability of detecting muons and P_n for detecting noise signals

TABLE I

JENSEN-SHANNON TEST, IN %, FOR THE MUON s_i SAMPLES.

s_1	s_2	s_3	s_4	s_5	s_6	s_7	s_8	s_9	s_{10}	s_{11}
99	100	95	63	33	32	48	72	89	97	99

to the pulse peak. This result also reveals that the number of samples used (11) could be less, as muon samples with *pdf* similar to the noise *pdf* do not provide useful information for signal discrimination. Nevertheless, this will be left for a future study.

Several studies concerning the TileCal response for muons showed that the muon energy distribution follows a Landau convoluted with Gaussian distribution [18]. As the signal pulse has an intrinsic dependence on the deposited energy, samples whose distributions are considerably different than noise should follow a distribution similar to the energy distribution. Nevertheless, the Gaussian approach (which is not far from the actual energy distribution for low signals [18]) was implemented, as it simplifies the design of the discriminators (attractive in online implementations).

1) Principal Component Analysis: The Karhunen-Loève representation of digital signals can be achieved using principal component analysis (PCA) [14]. The design of the stochastic approach discriminator requires the PCA to be performed over the muon signals without the presence of noise. This is unrealistic in many applications, and the PCA was evaluated from received signals under the H_1 hypothesis. Furthermore, PCA can also be used to compact the information by ranking the principal components (PC) according to their variance and excluding components with insignificant variance, which is attractive to L1 (speed).

Figure 4 shows the charge curve for the PCA extracted from the summed muon signals at η = 0.15, using the development set only. It can be seen that the first PC has nearly 70 % of the total variance. Signals from muons impinging the detector at other η also presented similar behavior.

V. SIMULATION

Figure 5 shows the ROC curves (Receiver Operating Characteristics) [12] for different η coordinates, estimated from the

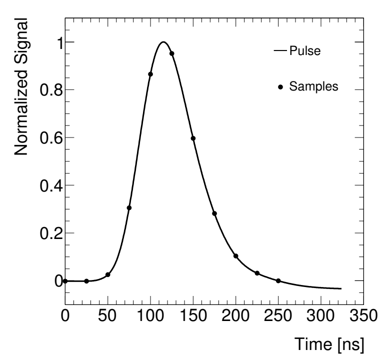

Fig. 3. Summed signal pulse shape seen at $\eta = 0.15$.

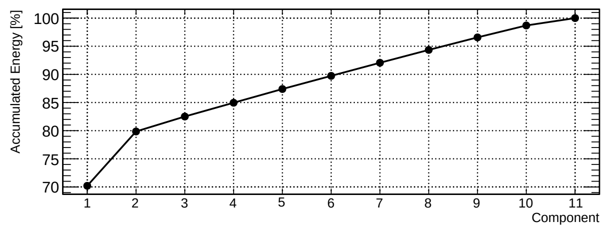

Fig. 4. Charge curve for PC extraction from muons impinging at $\eta = 0.15$.

evaluation set. Note that the performance improves according to η, as expected because the SNR also improves with η [11]. Table II shows the maximum SP index achieved for each design. It also shows the performance using a threshold discriminator over the digitized samples, which is a commonly used discriminator in high-energy physics experiments. It can be seen that the discriminators using the matched filter approach achieve better results with respect to the threshold detector. As matching to the mean value is as good as the stochastic design, the simpler discriminator is preferable for online implementation. Another possibility is to retain only the first PC in the Gaussian signal detection approach.

VI. Conclusions

Matched filter based efficient discriminators were designed for online muon triggering with the ATLAS L1 online trigger system. Such discriminators operate over TileCal muon signals, using calorimeter energy information to trigger on muons. The muon signals are summed up at the muon receiver in order to increase the SNR. Afterwards, they are digitized and stored at a FPGA. As the TileCal noise is not white, a whitening stage is designed for the receiver in order to correctly implement the matched filter based discriminators. FPGA implementation of such a discriminating system is planned to be tested.

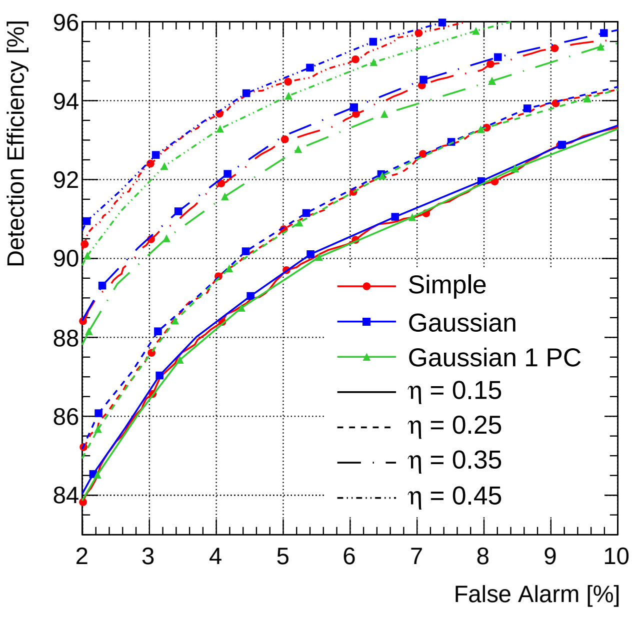

Fig. 5. ROC curves for the designed discriminators.

TABLE II

Maximum SP index (in %) for each discriminator.

η	Discriminators			
	Threshold	Matched Filter		
		Simple	Gaussian	Gaussian 1 PC
0.15	87.56	92.31	92.34	92.24
0.25	88.09	92.86	92.90	92.83
0.35	88.88	94.00	94.05	93.77
0.45	89.73	94.85	94.87	94.61

Acknowledgment

The authors are thankful for the support that has been provided to this work by CNPq, FAPERJ and RENAFAE (Brazil), and CERN. We would also like to thank our colleagues from the ATLAS TileCal and TDAQ groups for all the support and interesting discussions concerning the studies presented here.

References

[1] G. Watts, "Review of triggering," *IEEE Nuclear Science Symposium*, vol. 1, no. 50, pp. 282–287, October 2003.

[2] G. Aad et al., "The ATLAS experiment at the CERN Large Hadron Collider," *Journal of Instrumentation*, vol. 3, no. S08003, 2008.

[3] R. Wigmans, *Calorimetry: energy measurement in particle physics*. Oxford: Clarendon Press, 2000.

[4] K. Kordas et al., "The ATLAS data acquisition and trigger: concept, design and status," *Nuclear Physics B - Proceedings Supplements*, vol. 172, pp. 178 – 182, 2007.

[5] ATLAS/Tile Calorimeter Collaboration, "Tile calorimeter technical design report," 1996, CERN/LHCC 96–42.

[6] F. Ariztizabal et al., "Construction and performance of an iron-scintillator hadron calorimeter with longitudinal tile configuration," *Nuclear Instruments and Methods in Physics Research Section A*, vol. 349, pp. 384 – 397, 1994.

[7] K. Anderson et al., "Design of the front-end analog electronics for the ATLAS tile calorimeter," *Nuclear Instruments and Methods in Physics Research A*, vol. 551, pp. 469–476, 2005.

[8] A. Cerqueira et al., "Analog system for building the first-level triggering signal provided by the hadronic calorimeter of ATLAS detector," *Nuclear Instruments and Methods in Physics Research Section A*, vol. 570, pp. 117–125, 2007.

[9] T. Ciodaro et al, "A receiver system for the TileCal muon signals," vol. 1. Conference Record for IEEE Nuclear Science Symposium, 2009, pp. 1–8.

[10] A. Nisati, "Fake Level-1 muon trigger rates in the ATLAS experiment," CERN, Geneva, Tech. Rep. ATL-DAQ-98-123, 1998.

[11] P. Adragna et al, "Testbeam studies of production modules of the atlas tile calorimeter," *Nuclear Instruments and Methods in Physics Research, A*, vol. 606, pp. 362–394. 73 p, 2009.

[12] H. van Trees, *Detection, estimation, and modulation theory part I*. John Wiley & Sons, 2001.

[13] ——, *Detection, estimation, and modulation theory part III*. John Wiley & Sons, 2001.

[14] I. T. Jolliffe, *Principal component analysis*. Spring-Verlag, 2002.

[15] J. Tront, *PSpice for basic circuit analysis*. McGraw-Hill, 2005, vol. 2.

[16] A. R. dos Anjos, et al., "Neural triggering system operating in high resolution calorimetry information," *Nuclear Instruments and Methods in Physics Research Section A*, vol. 559, no. 1, pp. 134–138, 2006.

[17] J. Lin, "Divergence measures based on the shannon entropy," *IEEE Transactions on Information Theory*, vol. 37, pp. 145–151, 1991.

[18] T. Davidek et al., "Parametrization of the muon response in the Tile calorimeter," CERN, Geneva, Tech. Rep. ATL-TILECAL-97-114, 1997.